Application of extensional models to the Northern Viking Graben

JOHN P. GILTNER

Giltner, J. P.: Application of extensional models to the Northern Viking Graben. *Norsk Geologisk Tidsskrift*, Vol. 67, pp. 339–352. Oslo 1987. ISSN 0029-196X.

Subsidence curves corrected for compaction, estimated water depths of deposition, and changes in sea level from the Northern Viking Graben are matched to a uniform, two-phase, time-dependent extensional model. Total subsidence along the graben axis suggests a total extension of approximately 1.8, consisting of a Triassic extension of 1.5 and a Late Jurassic extension of 1.2. Within the graben, the model predicts subsidence very well, but the flanks are problematic. A more complicated model involving depth dependent stretching, mantle convection, or isostatic uplift of individual fault blocks may be needed to explain the uplift/non-subsidence of the graben flanks during rifting. Geometry of rotated fault blocks in the area accounts for extension of between 1.1 and 1.3, which is consistent with the Late Jurassic event. Although Triassic faulting is clearly seen on the eastern margin of the basin, early phase faulting in the graben axis has probably been rotated by the later tectonic activity and is not clearly imaged due to its depth and orientation. Crustal thinning determined from recent deep reflection and older refraction profiles suggest an extension of approximately 2.0, which is compatible with the observations of total subsidence.

John P. Giltner, University of Texas at Austin, Institute for Geophysics, 4920 North IH 35, Austin, Texas 78751 USA.

The Viking Graben is the northern portion of the generally north–south trending graben system of the North Sea. Underlain completely by continental crust, this oil productive region may be classified as an interior fracture basin (Kingston et al. 1983) or, in Bally's (1984) terms, a cratonic rift basin. Large rotated fault blocks, which provide the major hydrocarbon trapping mechanism, are characteristic features of this area. Recently, the assumption that the Northern Viking Graben is a typical extensional basin has been challenged (Beach et al. 1987) because of the discrepancy between estimates of extension from basin subsidence, crustal thinning, and fault displacement.

Previous attempts to model the North Sea as an extensional basin have concentrated on the Central Graben. Stretching models predict a certain amount of subsidence, crustal thinning and fault displacement for a given amount of lithospheric extension (McKenzie 1978). Sclater & Christie (1980) made estimates of extension by analyzing post mid-Jurassic subsidence observed in drill wells. Using seismic refraction data, Barton & Wood (1984) showed that estimates of crustal thinning beneath the Central Graben were compatible with estimates of extension from subsidence observations since Jurassic time. Finally, Sclater et al. (1986) considered the effects of earlier Permian and Triassic phases of rifting. Probably the major criticism to the application of extensional models to the North Sea has been that measurements of extension on observed faults have been consistently much smaller than extension estimated from crustal thinning and basin subsidence (Ziegler 1983). In addition, salt diapirism, thick Permian sediments, Jurassic/Cretaceous erosion, basin inversion, and strike slip faulting have made the analysis in the Central Graben excessively complex.

The Northern Viking Graben appears to display extensional tectonics in a more simplified and more easily observable form since it is north of the Permian salt basins; it has not experienced extensive uplift and erosion during the Mid Jurassic, and is further north of the major compressional effects of the Alpine orogeny (Fig. 1).

Besides being a good place to test the stretching models, the Northern North Sea is of enormous economic importance. With estimated recoverable reserves of 16 billion barrels of oil, the Northern Viking Graben is the most significant oil province in Western Europe (Ziegler 1977). The discovery of the super-giant Troll gas field in 1979 has made the region a crucial gas producing

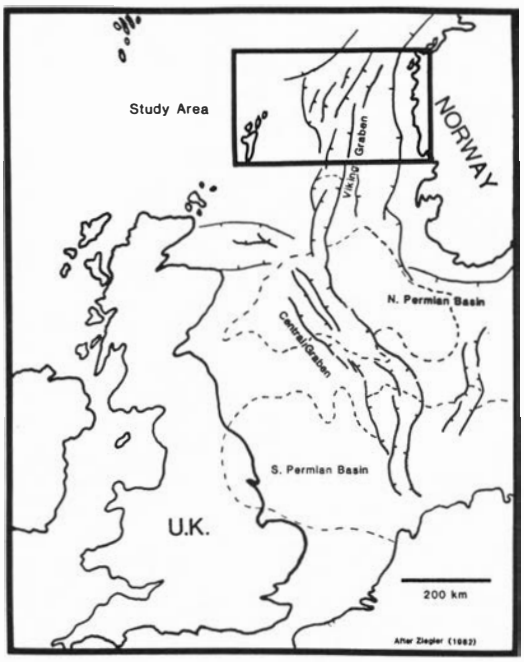

Fig. 1. Location of study area in relation to Central Graben and Permian salt basins.

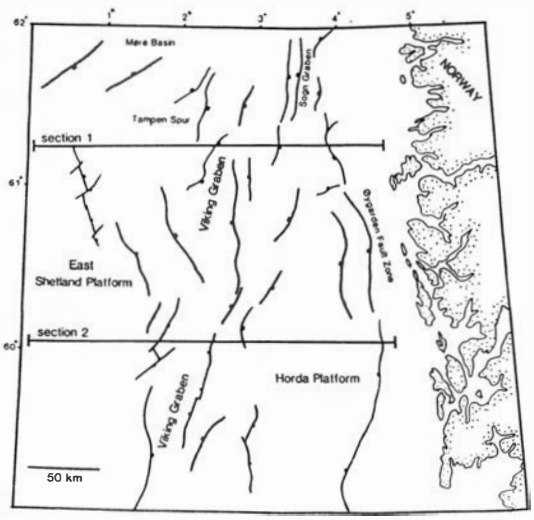

Fig. 2. Map of tectonic elements with locations of analyzed depth sections. Northern cross section is named Viking 1, southern is Viking 2.

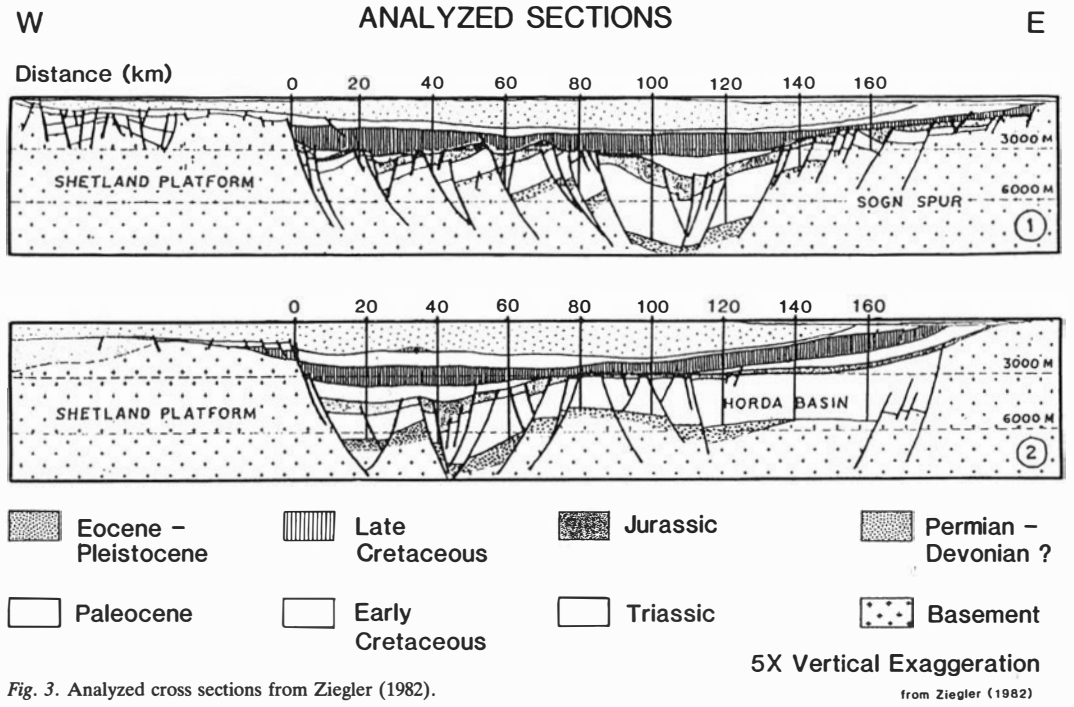

Fig. 3. Analyzed cross sections from Ziegler (1982).

province as well. A thorough understanding of the tectonic and sedimentologic development of this basin is of obvious importance.

In this analysis, careful observations of the subsidence history of two depth converted profiles from the Northern Viking Graben (Figs. 2, 3) are compared with predictions from a uniform, two-phase, time-dependent extensional model. The first part of the analysis involves constructing geohistory curves and obtaining subsidence observations from the Northern Viking Graben. In the following section, the quantitative extensional models are introduced. From these theoretical models, predictions of basin subsidence may be made by inputting certain magnitudes and timings for extensional events. Subsidence observations are then compared to the predictions of a model which has been constrained by the geologic history of the basin. Estimates of extension from crustal thinning and fault displacement may then be compared with the estimates from the subsidence analysis.

Subsidence observations

The amount of and manner in which subsidence in a sedimentary basin occurs may be determined by examining well and seismic data. Burial, geohistory, or subsidence curves are commonly used to display this data (Van Hinte 1978; Steckler & Watts 1978). Depth to a certain horizon, basement in this analysis, is plotted against time. Simple burial curves require thicknesses of selected sedimentary horizons and their respective age dates. More detailed and realistic subsidence curves require more complex sets of data such as water depths of deposition, eustatic changes in sea level, and corrections for compaction. The effect of each of these factors will be discussed in the following observations from two depth sections from the Northern Viking Graben (Fig. 2).

The general geologic history of the North Sea and the Northern Viking Graben has been well documented (Ziegler 1981, 1982; Badley et al. 1987). The basin is underlain by metamorphic basement consolidated during the Caledonian Orogeny (Silurian). Devonian basins are found along the western Norwegian coast and on the Shetland Platform, but their extensions offshore are unproven. Likewise, Permian sediments are very important in the Central and Southern North Sea, but the presence of Permian sediments north of 60 degrees is not well recorded. For these reasons, the modeling of this basin will not incorporate pre-Mesozoic tectonism and sedimentation. Thermal effects of possible Paleozoic, especially Devonian, tectonism are assumed to have completely decayed before the onset of Mesozoic extension.

Uncorrected subsidence curves may be derived by inputing only two sets of data: (1) age of sedimentary horizons, (2) depth to sediment horizons (sediment thicknesses). The high density of drilling in the North Sea has brought about a fairly detailed time scale for the area. Selected sedimentary horizons and their age dates are taken from Ziegler (1982) and Harland et al. (1982) (Fig. 4).

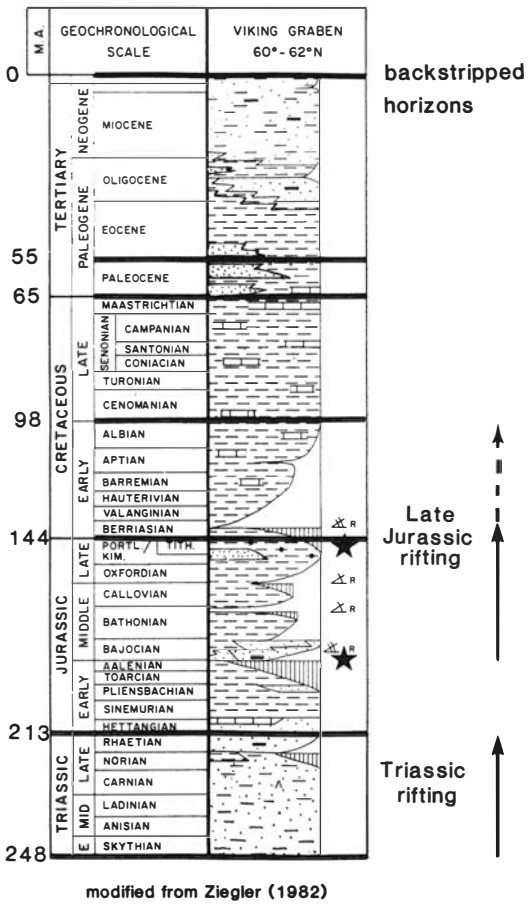

Fig. 4. Generalized tectonic/stratigraphic column from the Northern Viking Graben highlighting backstripped horizons and their age dates.

Originally, well data were used almost exclusively in acquiring stratigraphic thicknesses for subsidence analysis (Steckler & Watts 1978; Wood 1981). A major problem with well data is that it gives us information only in selected areas which are commonly clustered around structurally anomalous locations. Sawyer (1986) has shown the pitfalls of gathering subsidence data from structurally complex basement topography. In addition, drill wells commonly do not penetrate the full sedimentary section. For this reason, depth converted seismic sections (constrained by well data) published by Ziegler (1982) are used to obtain depths to dated horizons. Seismic profiles have the added advantage of enabling subsidence data to be gathered along an entire section. Stratigraphic thicknesses for subsidence analysis are extracted at 20 km intervals along each profile (Fig. 3). Well and seismic data are ideally combined in order to get the best subsidence analysis possible. Wells give us the detail, while seismic gives us the coverage needed.

In sedimentary basins such as the North Sea, subsidence is caused by three major modes: (1) crustal stretching, (2) thermal cooling, (3) sediment loading. In order to determine tectonic sub-

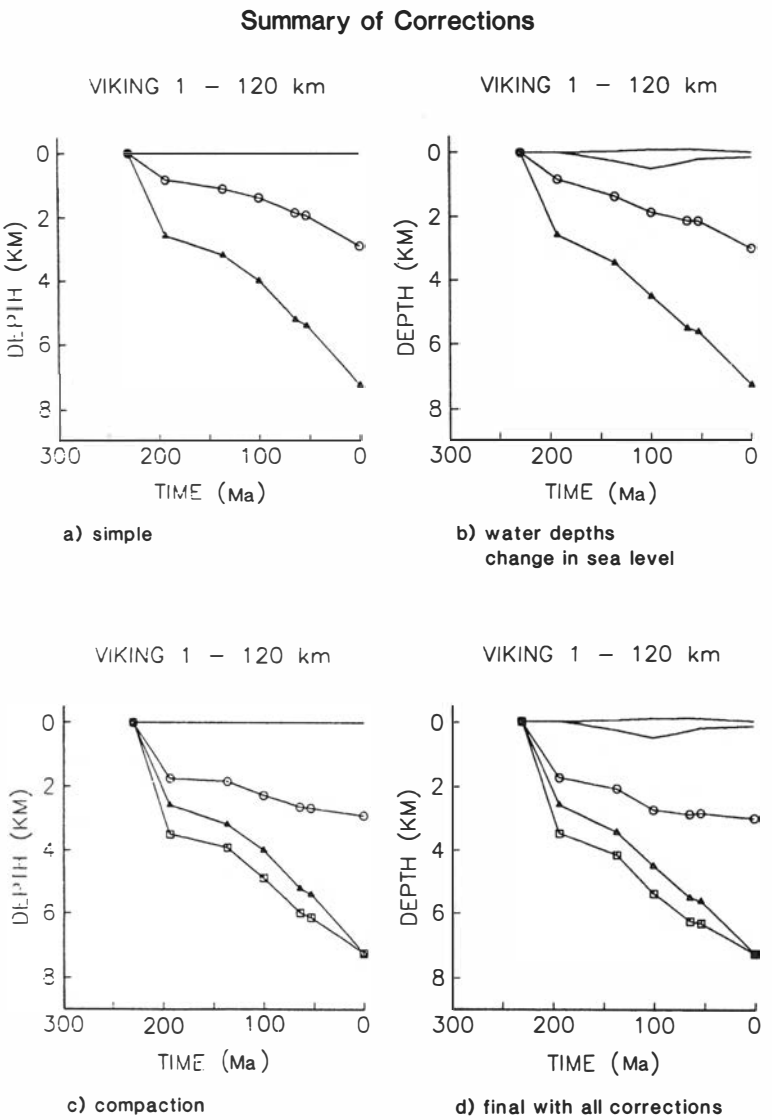

Fig. 5a–d. Subsidence curves and corrections for one backstripped point (cross section 1 at 120 km along the profile). Lines at the top of the plots show estimated water depths and eustatic changes in sea level, circles show waterloaded basement assuming local isotasy, triangles show basement depth uncorrected for compaction, and squares show basement depth corrected for sediment compaction.

sidence, which consists of subsidence due to crustal stretching and thermal cooling, the effect of sediment loading must be removed. This correction may be made by assuming either local isostatic or flexural loading of the lithosphere. Watts (1982) argues that an Airy type model is adequate during early rifting, while flexural loading becomes more important as a passive margin develops. Gravity modeling in the Central Graben by Barton & Wood (1984) also supports an isostatic loading mechanism.

Average sediment density (ρ_s) used in the calculations is computed by averaging the density of each lithologic thickness by assuming a porosity vs. depth function taken from Sclater & Christie's (1980) analysis in the Central Graben. Present average sediment densities for the sediment column at positions along the graben axis are calculated to be 2.3–2.4 g/cm^3. This calculation is performed for each point in time plotted on the subsidence curve. The sediments are isostatically unloaded following Steckler & Watts (1978) and the water loaded basement curve is plotted along with the sediment loaded basement curve in Fig. 5a.

Water depth of deposition and changes in sea level may be very important factors in analyzing basin subsidence (Steckler & Watts 1978; Wood 1981). Water depths of deposition of the selected sedimentary horizons for this study were obtained from P. A. Ziegler and O. Skarbø (personal communication) and supplemented by paleogeographic maps from Ziegler (1982) and Barton & Wood (1984). These depths represent a best estimate of long-term average values, since only first-order variations in water depth are necessary for this analysis. The diameters of the circles on the subsidence plots represent an uncertainty of ±150 m in the water depth estimates.

The shape of the eustatic curve utilized in this analysis was taken from Vail et al. (1977), assuming a conservative maximum eustatic rise of 100 m above present sea level during the Late Cretaceous (Watts & Steckler 1979). Although the precise magnitude of maximum eustatic sea level is debatable (Vail et al. (1977) suggest a maximum of 350 m), some correction should be made.

The basement subsidence curves must be adjusted for these water level effects. Sediment unloading calculations are also slightly different when water level effects are incorporated into the model. The same isostatic principles apply, but two new variables are entered into the calculations (Fig. 5b).

In order to obtain accurate subsidence observations, the effect of sediment compaction due to burial must be addressed. Sediment thicknesses (S_t) measured in a stratigraphic section today do not represent actual sediment thickness at the time of deposition (S_t*). For this reason, a quantitative method for calculating decompacted sediment thickness must be utilized (Sclater & Christie 1980). The initial porosities and compaction constants for different lithologies are taken from Sclater & Christie's (1980) backstripping analysis in the Central Graben. The lithologies for the Viking Graben profiles used in this study were derived from Ziegler's (1982) paleogeographic maps.

Fig. 5c shows the effect of compaction on basement subsidence (water level effects have been ignored in order to better display the compactional effects). The isostatic loading calculations are identical to the simple burial curve calculations, except now the average sediment density (ρ_s*) must be recalculated each time the sediments decompact. This computation results in a lower sediment density than in the simple burial curve calculations where we did not take compaction into account.

The final burial curve takes into account the effects of water depth of deposition, sea-level fluctuations, and compaction (Fig. 5d). The unloaded or tectonic subsidence curves will be compared to the theoretical curves derived from the time-dependent stretching model.

A few interesting points can be noticed by observing the four subsidence curves derived using the calculations described above (Fig. 5). Each curve begins at the same point (248 Ma, 0 depth) and ends at the same point (0 Ma, 7200 m-loaded, 3000 m-unloaded). The only difference in the curves is the subsidence path the basement follows. Therefore, water depths, eustatic changes, and compactional effects are crucial in determining the path of basement subsidence, but not the final subsidence observed. This is analogous to the calculation of synthetic subsidence curves to be developed in the next section. The final subsidence of the synthetic curve is solely a function of the total amount of extension, not the number and duration of extensional events experienced.

Subsidence curves from each selected point along the Viking Graben cross sections have been

constructed. The total subsidence is clearly the greatest in the central portion of the graben where sediment loaded basement is 8 km deep and the calculated water loaded basement is about 3 km deep. On the flanks of the graben sediment-loaded basement depth averages 4–5 km, while water-loaded basement depth is around 2 km. In order to test our model of basin formation, these subsidence observations must now be compared to the predictions of the time-dependent extensional model.

Extensional models of basin formation

A simplified model of extensional basin formation was mathematically formulated by McKenzie (1978). A relatively light crust overlying more dense mantle material was assumed to have been stretched instantaneously and uniformly with depth. Hot asthenosphere rises isostatically upward to replace the thinned lithosphere and then cools and contracts with time. The effects on four separate observations may be analyzed and related to an extensional parameter β (where β is equal to the ratio of basinal area or length after stretching to that before stretching): (1) subsidence, (2) heat flow, (3) crustal thinning, (4) brittle extension on faults.

Subsidence observations and predictions are the major topics of this analysis, but the other characteristics may be just as important in estimating the amount of extension in a basin. The relation between heat flow and extension is very important in young basins, but becomes more erratic and of lesser use in older basins such as the North Sea. For this reason, heat flow will not be discussed in this analysis. Crustal thinning deserves detailed attention since it is the absolute reason for development of an extensional sedimentary basin. Finally, estimates of brittle extension have received much attention recently (White et al., in press) since it is the major impediment to acceptance of the extensional models (Ziegler 1983).

Some theoretical subsidence curves for varying amounts of extension assuming instantaneous stretching and an initial crustal thickness of 35 km are shown in Fig. 6a. Equations for initial and thermal subsidence are taken from McKenzie (1978) with geophysical parameters from Parsons & Sclater (1977). Although the model is elegantly presented, the synthetic subsidence curves reveal the assumption of instantaneous stretching to be unreasonable, especially in the case of the North Sea where active extension occurred over many tens of millions of years. The basics of this instantaneous stretching model are essential in understanding time-dependent mechanics, however.

The time-dependent extensional model takes into account the duration of stretching in the idealized model (Jarvis & McKenzie 1980). During stretching over finite time (Δt), some of the subsidence caused by thermal cooling occurs. Although final subsidence (S_∞) is equivalent in both the instantaneous and finite stretching models, the proportion of syn-rift and post-rift varies.

The mathematics of solving for syn-rift and post-rift subsidence become quite complex, therefore, a simpler method for deriving these values has been derived by Sclater et al. (1986). Synthetic subsidence curves may be constructed by inputting selected values for initiation of rifting, termination of rifting, amount of extension and initial crustal thickness. An example of some time-dependent subsidence curves is shown in Fig. 6b. Each curve has an extensional parameter β of 2.0, but the duration of stretching varies from 0 Ma to 200 Ma. All the curves begin at zero depth at 248 Ma and all will finish at a depth of 4.3 km, although the slow stretching curve will get there after a longer period of time.

Two separate periods of extension may also be modeled. The initial stretching event thins the crust and causes subsidence. A subsequent extensional event will start with a new crustal thickness which is computed by knowing the extent of the first event. Subsidence due to the second event is added to the subsidence caused by the first tectonic phase. An example is shown in Fig. 7 where an initial extension of $\beta = 2.0$, $\Delta t = 50$ Ma is followed by an event with $\beta = 1.5$, $\Delta t = 20$ Ma.

Matching of model to observations

Final corrected subsidence curves from the Northern Viking Graben must now be compared with the subsidence predicted from the model. The timing and duration of the extensional events used in constructing the theoretical subsidence profiles must be constrained by the documented geologic history of the area. Badley *et al.* (1984, 1987) have recognized two major episodes of rifting in the study area, the first during the Triassic and the

second during the Late Jurassic/Early Cretaceous.

The initiation of the first rift event is dated at Late Permian or Early Triassic by sediments penetrated in deep boreholes in the region. Block faulting of crystalline basement is observed on seismic sections from the eastern margin of the basin. This extensional event is poorly constrained since basement reflections may not be positively identified throughout the central portion of the graben (from 1 40′E to 3 30′E). However, the poor control of this event should not be confused with its importance in explaining the subsidence history of the basin. The central portion of the Viking Graben and the Horda Platform each contain approximately 3 km of Triassic sediments (about 4 km decompacted). In this analysis, I have taken the initiation of the early tectonic event at earliest Triassic time (248 Ma). Although the rifting was probably sporadic, the termination of tectonism, which is again poorly constrained, is taken at the end of Triassic time (213 Ma).

Evidence for the thermal subsidence associated with the Triassic rifting has been well documented (Badley et al. 1987). Lower Jurassic sediments gradually thicken toward the basin center, with some local thinning on footwall blocks. Regional correlation of Lower to Middle Jurassic strata suggests that no significant structural topography was present at this time.

The second major rift episode beginning in Middle Jurassic time (169 Ma) is much more obviously recognized and has been widely publicized (Sclater & Christie 1980; Barton & Wood 1984). Onlapping syn-rift deposits of post Brent age (Bathonian) mark the initiation of block faulting and rotation of older strata. Limited erosion of the Brent Group indicates that the crests of some rotated blocks may have been emergent, although Ziegler (1981) believes erosion/non-deposition during Early Cretaceous time to be due to submarine contour currents. No regional uplift or pre-rift doming, besides local uplift on footwalls, accompanied the extension (Badley et al. 1987). Observed faulting in the two cross sections probably occurred during this rift phase. Most of the tectonic activity ceased during the earliest Cretaceous (Berriasian 130 Ma), although intermittent tectonism probably continued into middle Cretaceous time. The termination of this second rift phase is taken at 98 Ma in constructing the predicted subsidence.

A second phase of thermal subsidence followed this later extensional event leading to a symmetrical Cretaceous/Tertiary sag basin. This thermal subsidence may be a combination of both tectonic events if the thermal anomaly due to the Triassic event has not completely decayed by mid-Jurassic time. Most previous workers have assumed that most of the post mid-Jurassic subsidence is due only to the Late Jurassic tectonic

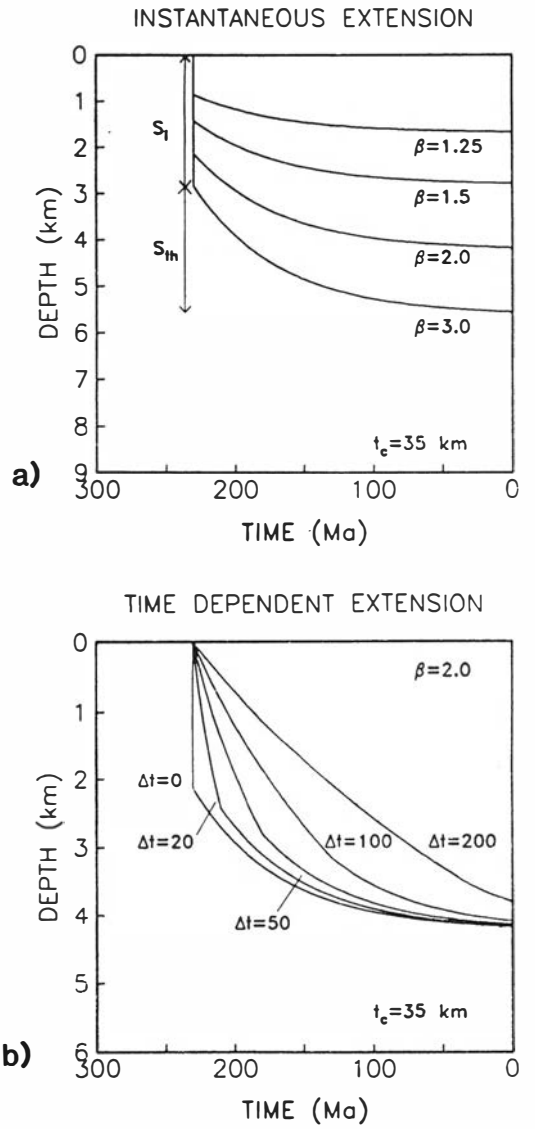

Fig. 6a–b. Plots of theoretical subsidence calculated from (a) McKenzie's (1978) uniform, instantaneous extensional model, and (b) Jarvis & McKenzie's (1980) uniform, time-dependent extensional model.

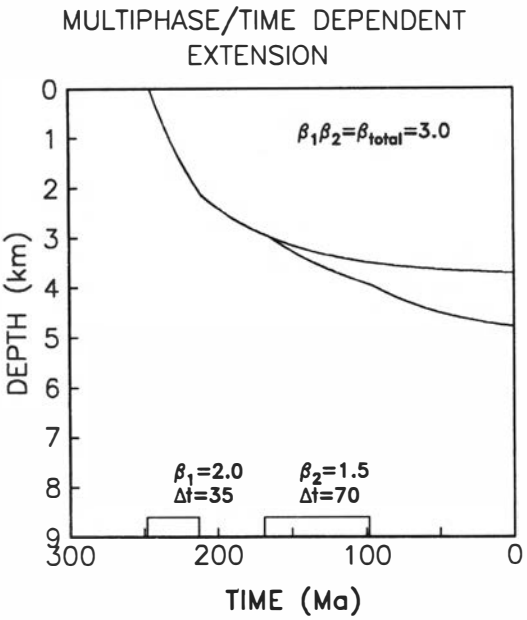

Fig. 7. Subsidence predicted by a uniform, two-phase, time-dependent model consisting of a Triassic phase of rifting followed by a Late Jurassic/Early Cretaceous tectonic phase.

event (e.g. Barton & Wood 1984, Badley et al. 1987). This may not be the case if the Triassic event is of sufficient magnitude.

A uniform, two-phase, time-dependent model consisting of an early event lasting from 248 Ma to 213 Ma and a later event lasting from 169 Ma to 98 Ma has been matched to the observations of subsidence compiled in the previous section. An example of a synthetic subsidence curve with these constraints is shown in Fig. 7. The initial crustal thickness is taken as 35 km following estimates for the Fenno-Scandian shield from Calcagnile (1982) and Sclater et al. (1986).

Matches of predicted subsidence to observed subsidence for locations along each profile are shown in Fig. 8a–8d (backstripped profiles are shown again in Fig. 3 for reference). Positions within the graben proper (Fig. 8a) show a very good fit of predicted and observed subsidence. The match was made by first fitting the Triassic subsidence and then adding a Late Jurassic phase of sufficient magnitude to fit the younger portion of the curves. Adjustments were made to the relative magnitudes of the two events until a satisfactory match was made. The Late Jurassic phase is of considerably lesser magnitude at all of the backstripped positions within the graben. In addition, these plots reveal that a significant portion of the post Mid-Jurassic subsidence is due to thermal contraction from the earlier Triassic rift event.

Results from the Horda Platform on the eastern part of the southern cross section are shown in Fig. 8b. In this portion of the basin, a single Triassic rift event can explain almost all of the observed subsidence history. Subsidence from the easternmost position does not display any effect at all of Late Jurassic tectonism. As in the graben areas, a simple uniform extensional model is sufficient to predict basin subsidence.

Problems in the matching occur when we look at the graben flanks. Fitting of curves from the western flank of the Viking Graben (Tampen Spur) is shown in Fig. 8c. In this case, the immediate subsidence predicted from the model during the Late Jurassic rift phase is not noticed in the observations. Non-subsidence is the rule in this area, not regional uplift. The mismatch is accentuated at locations on the crests of the rotated fault blocks (viking 1–20 km). Structurally low positions, such as viking 1–60 km, also display the same mismatch, but to a lesser degree. The majority of exploratory wells are drilled precisely where the mismatch of the model to the observations is the greatest, therefore serious errors may result from relying completely on well data in subsidence modeling. The continuous profile provided by seismic sections is a distinct advantage.

The eastern flank of the graben (Sogn Spur, Utsira High) shows the same mismatch as on the western flank (Fig. 8d). Non-subsidence during Late Jurassic/Early Cretaceous times at these locations cannot be explained by a simple uniform extensional model. The model predicts subsidence and therefore deposition during the Early Cretaceous. More needs to be learned about Early Cretaceous paleogeography in order to understand water depth and sediment deposition during this period.

Uplift of graben flanks during rifting has been noted in studies from the Gulf of Suez (Steckler 1985), the Pannonian Basin (Royden et al. 1983), the Viking Graben (Hellinger & Sclater 1983), and the mid-Norway margin (Bukovics & Ziegler 1985). Most explanations of this phenomenon involve a depth dependent stretching model where the lower lithosphere is stretched by a greater amount than the overlying crust (Royden & Keen 1980). The effect of this model is to

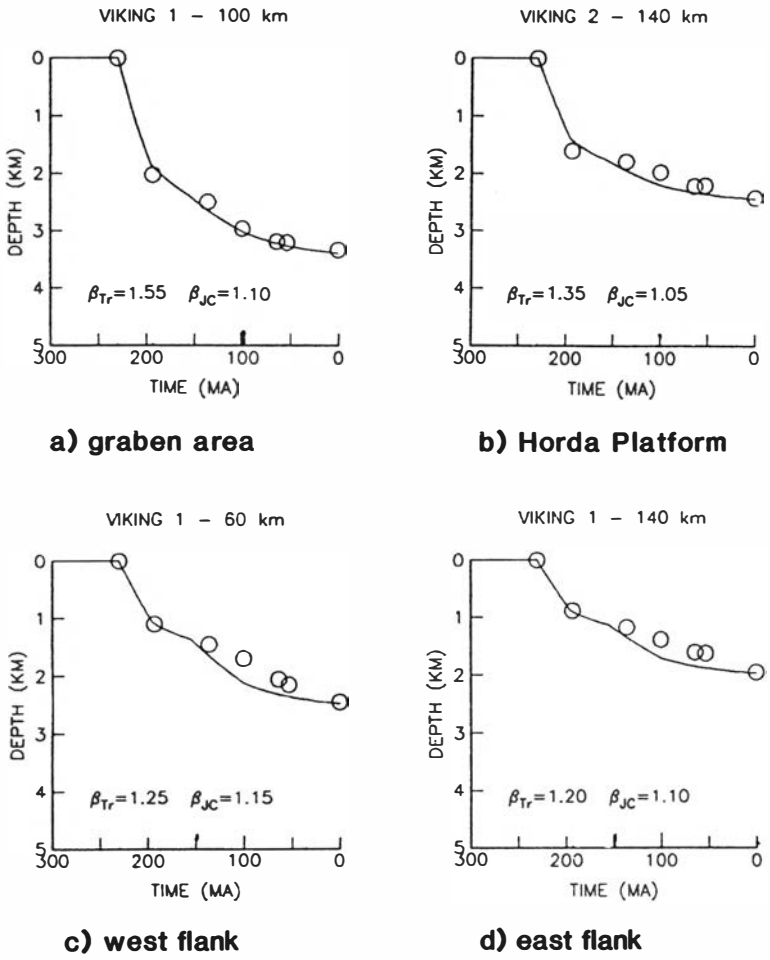

Fig. 8. Representative matches of predicted and observed subsidence from various tectonic environments across the two profiles. The thermal subsidence due to Triassic rifting has not completely decayed before the onset of the second rift event, especially along the graben axis. Uplift of the graben flanks during rifting causes mismatch of predictions and observations. Plots are named by cross section (Viking 1 or 2) and distance along the profile.

introduce more heat from the upwelling asthenosphere into the basin. Thermal expansion of the lower lithosphere beneath the graben flanks exceeds or at least counteracts the initial subsidence due to crustal thinning. Conservation of total lithospheric mass and conceptual reason why and how depth-dependent stretching occurs are commonly cited problems with the model. In a slightly different approach, Buck (1986) and Steckler (1985) envision mantle convection due to large horizontal thermal gradients at depth to be responsible for the input of heat into the rift flanks. Passive upwelling of asthenosphere material to the crust/mantle interface during rifting has also been cited as the reason for uplifted flanks (Neugebauer 1983). In summary, we know that uplift/non-subsidence of graben flanks during rifting occurs, but we don't know exactly why (Sclater & Celerier 1987).

Two-dimensional plots of stretching factors for each cross section are shown in Fig. 9a–b. These values are derived from the best fit of predicted to observed subsidence. Magnitudes of extension for the Triassic and the Late Jurassic events are plotted below their respective positions on the cross section. Total extension, computed by taking the product of the two component phases, is also shown.

In section one, Triassic rifting is concentrated in the central portion of the graben. A maximum extension of 1.6 within the graben gradually falls off to 1.2 to the east and west. This distribution may be easily observed in the cross section by noting the very thick succession of Triassic sediments interpreted in the graben.

Section two to the south displays a different character for the Triassic event. Tectonism is more evenly distributed from west to east, con-

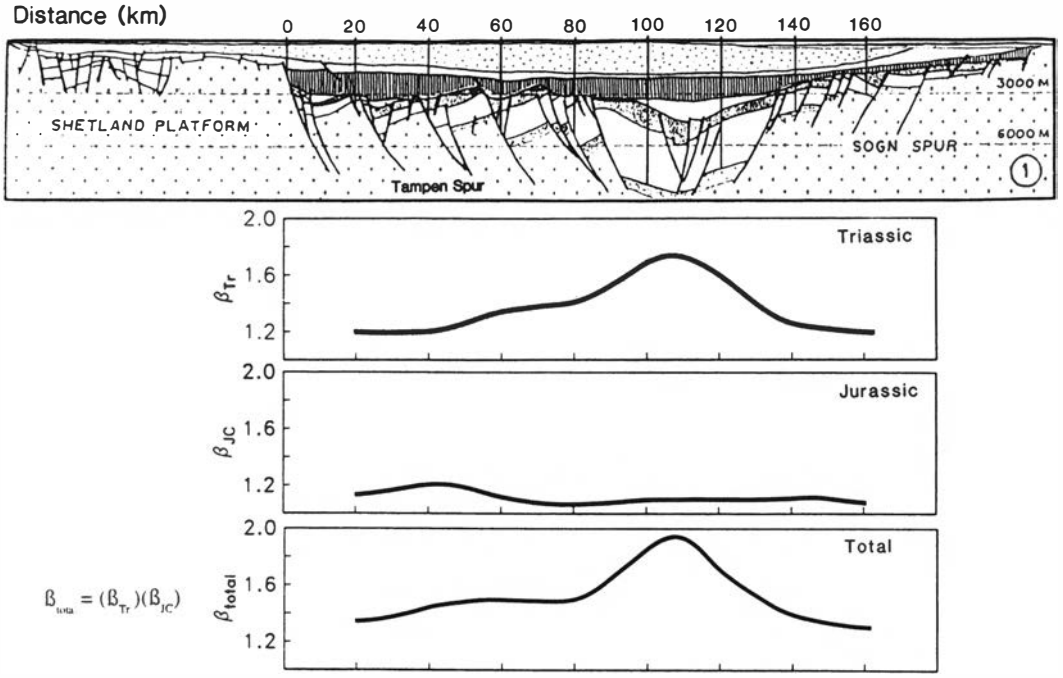

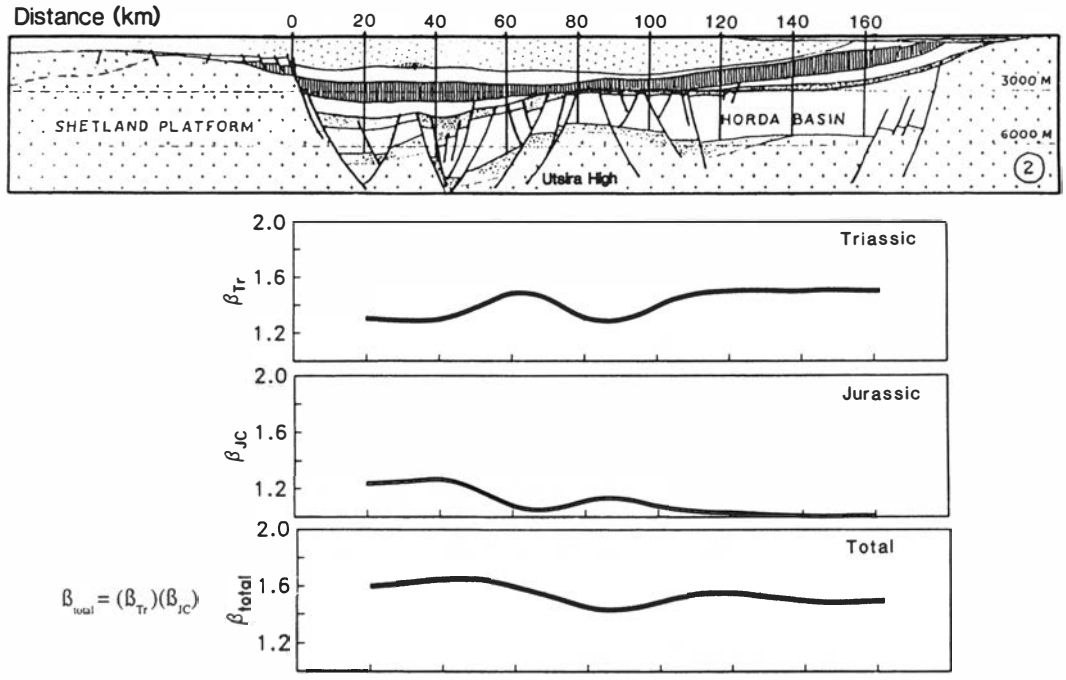

Fig. 9a–b. Two-dimensional display of estimates of extension for each rifting phase determined from subsidence analysis. Note the relatively small magnitude of the Late Jurassic rift event.

sisting of two Triassic basins: (1) Viking Graben (west), (2) Horda Basin (east). The thinning of Triassic strata over the Utsira High suggests that this basement feature was a topographic high which partially separated the Viking Graben from the Horda Platform during Triassic time. In this section, the maximum extension is approximately 1.4 both in the graben and the eastern basin.

The second extensional event is of much lesser magnitude in both sections, with a maximum extension of 1.2. Most of the Late Jurassic tectonism is concentrated in the western half of the study area, without good correlation to the graben axis. The density of the observed faulting appears to correspond with the magnitude of the second event. Faulting above basement is rare in the Horda Basin (section 2), and subsidence modeling indicates that Late Jurassic tectonic activity is very limited in this area. The Utsira High seems to shield the Horda Platform from Late Jurassic extension. Some workers (Badley et al. 1987) have suggested that the Horda Platform is underlain by abnormally light crustal material, such as a granitic batholith, which inhibits subsidence.

The total extension estimated from the subsidence analysis is dominated by the character of the Triassic rift event. This curve shows a maximum total extension of approximately 1.8 along the graben axis in the northern section. Total extension is again more evenly distributed in section two with a maximum extension of 1.55.

Estimates of extension from crustal thinning and fault geometry

In order to have good confidence in the validity of the stretching model, estimates of extension determined from the amount of crustal thinning beneath the graben should be compatible with estimates of extension from subsidence analysis. Stretching of the lithosphere should leave the crust thinned by the factor β beneath the basin, where final crustal thickness is given by: initial crustal thickness/β. This final crustal thickness will display the cumulative effect of both tectonic pulses, therefore estimates of extension from crustal profiles should be compared to the estimates of extension derived from the total present subsidence.

Seismic profiles, both refraction and deep reflection, are commonly utilized in resolving deep crustal structure (Barton & Matthews 1984). A combination reflection/refraction profile across the Viking Graben (Solli 1976) has been widely cited in the literature (Ziegler 1977). Assuming an initial crustal thickness of 35 km, and taking the same crustal thickness beneath the Norwegian mainland, extension beneath the center of the graben is calculated to be 2.0–2.3. The inferred extension decays to the east and west in much the same manner as the 2-D plot of total present-day subsidence. Estimates of extension from these two independent sources are very similar, providing excellent support for the fundamental idea of lithospheric stretching and subsequent cooling.

A more recent deep reflection line (Beach et al. 1987) shot across the Viking Graben displays the same general features as Solli's (1976) line. Maximum extension in the center of the graben is again calculated to be 2.0–2.3. These additional data provide considerably more confidence in deep crustal structure beneath the Viking Graben. Problems in reflection interpretation and velocity control make the analysis somewhat complex, but the generalized picture is quite clear. The crust beneath this basin is thinned to about half its original thickness, which is in good agreement with the subsidence data. The crust may be thinned by a greater amount than that suggested by the subsidence data because of possible Devonian extension (Beach 1985) not considered in the subsidence analysis.

Probably the major stumbling block to wide acceptance of the elegant stretching models has been the mismatch of extension measured from brittle faulting and extension determined from subsidence and crustal structure studies. Ziegler (1983) has shown that the observed faulting in the Central Graben accounts for only about 30% of the total extension estimated from subsidence analysis, although obtaining reliable estimates of extension from fault geometry is controversial (Jackson & McKenzie 1983). Better resolution of extensional faulting in the Viking Graben, due to the absence of salt cover, should allow more accurate estimates of extension to be made (White, pers. comm.).

A rough estimate of extension has been made by applying a simple domino-type model (LePichon & Sibuet 1981) to the rotated fault blocks observed in section one. Taking an average dip of 10 degrees for the rotated sedimentary strata and an average dip of 45 degrees for the bounding faults, extension is estimated to be 1.16. If the strata dipped at an angle of 15 degrees,

extension would be 1.22. Simple addition of the heaves on the observed faulting leads to a stretching factor of approximately 1.2. In all cases, estimates of extension from the faulting are much less than estimates from the subsidence and crustal thinning analysis. No matter what assumptions we make concerning dip of beds, dip of faults, compaction, etc., we cannot account for the total extension suggested by subsidence and crustal thickness data by the observed faulting.

From subsidence modeling, the amount of extension during the Later Jurassic phase of tectonic activity has been estimated to be about 1.10–1.20. This is strikingly similar to estimates obtained from the observed faulting. It appears that only the latest phase of tectonic activity is recorded in the seismically resolvable faulting. Rotation of the presently observed fault blocks and petroleum migration into these structures occurred during the Late Jurassic after relatively minor extension of approximately 20% ($\beta = 1.2$).

Triassic faulting is only positively identified on the eastern portion of the Horda Platform where the later Jurassic event is not prevalent. In the graben axis, Triassic faulting is not observed because of its depth and orientation. Initial graben faults formed during the Early Triassic have probably been rotated and refaulted a number of times during basin evolution. Rotation and refaulting of early phase normal faults has been documented to occur in the extensional regime of the Basin and Range, U.S. (Proffett 1977). Gibbs (1984) proposes that lock up of early extensional faults may occur after an extensional factor of around 1.5, although earlier lock up may occur. These early faults become increasingly more difficult to detect as extension progresses. The stretching model is found to be consistent with brittle faulting because only a small percentage of the faults associated with extension are presently observed.

Discussion

The detailed two-dimensional subsidence analysis of this study should be viewed in light of other recent attempts to quantify the structural evolution of the Northern Viking Graben (Badley et al. 1987; Beach et al. 1987; Beach 1985). Mismatch of stretching factors derived from subsidence data, crustal thinning, and brittle faulting has resulted in increasingly more complex models of basin formation. This work has shown that the estimates of extension derived from independent criteria are not totally inconsistent and a simpler extensional history is plausible.

Badley et al. (1987) calculated extension factors from three separate methods in their analysis: (1) displacement on observed faulting, (2) thickness of observed syn-rift sediments due to the Late Jurassic event, (3) post-Jurassic thermal subsidence. Observed faulting and thicknesses of syn-rift sedimentation both indicate stretching factors ranging from 1.05 on the basin margins to about 1.15 in the graben center. Estimates of extension from the thermal subsidence associated with the second rift episode vary from 1.15–1.35 on the basin margins to about 1.5 in the graben center. In their view, this significant discrepancy prohibits the application of a simple uniform extensional model. Calculation of extension from fitting the thermal portion of observed subsidence curves to subsidence predicted from theoretical models is brought into question.

The consistency of Badley et al.'s (1987) stretching factors derived from fault displacement and syn-rift sedimentation is similar to my estimates from simplistic calculations of fault geometry and from the subsidence analysis; therefore, extension by a factor of 1.1–1.2 is probably about right for Late Jurassic tectonism. In their work, the thermal anomaly associated with earlier Triassic rifting is assumed to have completely decayed before the initiation of the second rifting event. This is probably not the case, especially in the graben center where Triassic extension has a β of approximately 1.5–1.6. The addition of thermal subsidence associated with Triassic rifting to the post mid-Jurassic subsidence has caused overestimation of Late Jurassic extension in the Central Graben as well as the Viking Graben (Sclater & Christie 1980; Sclater et al. 1986).

Beach et al. (1987) invoke a strike-slip, pull apart basin system which developed during Late Jurassic tectonism to explain the discrepancy between stretching factors calculated from subsidence, crustal thinning, and brittle faulting. Their analysis of subsidence suggests a Mesozoic stretching factor of at least 3.0 beneath the graben axis, although LePichon & Sibuet (1981) estimate continental break-up to occur after extension close to that magnitude ($\beta = 3.2$). Crustal attenuation beneath the graben indicates extension by a factor of 2.0–2.3, as mentioned earlier in this paper. Triassic tectonism in a dominantly exten-

sional mode, which causes the observed crustal thinning, is followed by large-scale linked tectonics involving major strike slip displacements during the Late Jurassic (Beach 1985). The later phase of tectonic activity results in additional basin subsidence, but no additional crustal attenuation.

Although the evolution of the Northern Viking Graben is surely more complicated than pure regional extensional, predictions from a simple extensional model are generally consistent with the observations. Sclater et al. (1986) have reached the same general conclusion in the Central Graben. Strike slip faulting should be expected to occur concurrently with extension as so-called transfer faults (Gibbs 1984), although they are not reasons for basin formation.

Crustal detatchment models of extension developed from field studies in the Basin and Range of the U.S. (Wernicke & Burchfiel 1982) have been applied to the North Sea (Gibbs 1984; Beach et al. 1987). These models predict crustal thinning where the detatchment fault intersects the crust and lower lithospheric thinning where the detatchment intersects the lithosphere/asthenosphere interface. The detailed cross-sectional subsidence analysis in this study has shown that thermal subsidence associated with lower lithospheric stretching and initial subsidence associated with upper crustal brittle faulting are both generally centered along the graben axis. If extension along a crustal detatchment does occur in this area, symmetric initial and thermal subsidence must be accounted for.

Conclusions

Subsidence observations may be compared to subsidence predicted by theoretical stretching models in two basic ways: (1) match the subsidence history at a particular point in a basin, (2) compare total present-day subsidence with estimates of extension from independent observations. Both methods have been utilized in this study in order to obtain a better understanding of the structural evolution of the Northern Viking Graben.

First of all, it has been shown that a uniform, two-phase, time-dependent extensional model predicts subsidence history very well along the graben axis and on the Horda Platform. However, uplift/non-subsidence of the graben flanks during rifting suggests something more complicated may be happening at depth. Depth-dependent stretching, mantle convection, emplacement of an 'asthenolith', and isostatic uplift of footwalls have all been proposed to account for this phenomenon since it has been observed in numerous rift environments.

Secondly, estimates of extension from crustal thinning ($\beta = 2.0$) and estimates from total present-day subsidence ($\beta = 1.8$) beneath the graben axis are compatible. The 'additional' crustal thinning may have occurred during the development of Devonian basins in the area. From subsidence modeling, total basin extension in the graben center of 1.8 has been determined to consist of Triassic stretching by a factor of about 1.5 and a Late Jurassic extension of about 1.2. Measurements of observed faulting in the area indicate extension by a factor of around 1.1–1.2, which is consistent with the Late Jurassic phase of tectonism only. Faulting associated with Triassic rifting has been rotated and refaulted by later tectonic activity and is not resolvable on reflection seismic lines due to its depth and orientation.

Acknowledgements. – This material is based upon work supported under a National Science Foundation Graduate Fellowship. Support for participation in this conference has been generously supplied by the Department of Geological Sciences (University of Texas), J. G. Sclater and Nopec A.S. I wish to thank Nopec for access to their database over the summer and all the individuals who have made contributions to this work, especially H. Carstens. Reviews of the manuscript by B. Célérier and D. Sawyer and information on water depths of deposition from P. A. Ziegler and O. Skarbø have been extremely helpful.

References

Badley, M. E., Price, J. D., Dahl, C. R. & Agdestein, T. 1987: The structural evolution of the northern Viking Graben and its bearing upon extensional modes of basin formation, in press. *The Geological Society of London.*

Badley, M. E., Egeberg, T. & Nipen, O. 1984: Development of rift basins illustrated by the structural evolution of the Oseberg feature, block 30/6, offshore Norway. *Journal of the Geological Society of London 141*, 639–649.

Bally, A. W. 1984: Structural styles and the evolution of sedimentary basins. *AAPG short course notes*, Rice Univ., Houston, Texas. 238 pp.

Barton, P. J. & Matthews, D. H. 1984: Deep structure and geology of the North Sea region interpreted from a seismic refraction profile. *Annales Geophysicae 2*(6), 663–668.

Barton, P. & Wood, R. 1984: Tectonic evolution of the North Sea basin: crustal stretching and subsidence. *Geophysical Journal Royal Astronomical Society 79*, 987–1022.

Beach, A. 1985: Some comments on sedimentary basin development in the Northern North Sea. *Scottish Journal of Geology 21*, 4, 493–512.

Beach, A., Bird, T. & Gibbs, A. 1987: Extensional tectonics and crustal structure: deep seismic reflection data from the northern North Sea Viking Graben. *Geological Society of London, special publication*, in press.

Buck, W. R. 1986: Small scale convection induced by passive rifting: the cause for uplift of rift shoulders. *Earth & Planetary Science Letters 77*, 362–372.

Bukovics, C. & Ziegler, P. A. 1985: Tectonic development of the Mid-Norway continental margin. *Marine and Petroleum Geology 2*, 2–22.

Calcagnile, G. 1982: The lithosphere–asthenosphere system in Fennoscandia. *Tectonophysics 90*, 19–35.

Gibbs, A. D. 1984: Structural evolution of extensional basin margins. *Journal of the Geological Society of London 141*, 609–620.

Harland, W. B., Cox, A. V., Llewellyn, P. B., Pickton, C. A., Smith, A. G. & Walters, R. 1982: A geologic time scale. *Cambridge University Press.*

Hellinger, S. J. & Sclater, J. G. 1983: Some comments on two-layer extensional models for the evolution of sedimentary basins. *Journal Geophysical Research 88*, b10, 8251–8269.

Jackson, J. A. & McKenzie, D. P. 1983: The geometrical evolution of normal fault systems. *Journal of Structural Geology 5*, 471–482.

Jarvis, G. T. & McKenzie, D. P. 1980: Sedimentary basin formation with finite extension rates. *Earth & Planetary Science Letters 48*, 42–52.

Kingston, D. R., Dishroon, C. P. & Williams, P. A. 1983: Global basin classification system, *American Association of Petroleum Geologists Bulletin 67*, 12, 2175–2193.

LePichon, X. & Sibuet, J. C. 1981: Passive margins – a model of formation. *Journal of Geophysical Research 86*(B5), 3708–3720.

McKenzie, D. P. 1978: Some remarks on the development of sedimentary basins. *Earth & Planetary Science Letters 40*, 25–32.

Neugebauer, H. J. 1983: Mechanical aspects of continental rifting. *Tectonophysics 94*, 91–108.

Parsons, B. & Sclater, J. G. 1977: An analysis of ocean floor bathymetry and heat flow with age. *Journal Geophysical Research 82*, 803–827.

Proffett, J. M. 1977: Cenozoic geology of the Yerrington district, Nevada, and implications for the nature and origin of Basin and Range faulting. *Geological Society of America Bulletin 88*, 247–266.

Royden, L. & Keen, C. 1980: Rifting process and thermal evolution of the continental margin of Eastern Canada determined from subsidence. *Earth & Planetary Science Letters 51*, 343–361.

Royden, L., Horvath, F. & Rumpler, J. 1983: Evolution of the Pannonian Basin system. *Tectonics 2*(1), 63–90.

Sawyer, D. S. 1986: Effects of basement topography on subsidence history analysis. *Earth & Planetary Science Letters 78*, 427–434.

Sclater, J. G. & Célérier, B. 1987: Extensional models for the formation of sedimentary basins and continental shelves. *Norsk Geologisk Tidsskrift*, this volume, 253–267.

Sclater, J. G. & Christie, P. A. F. 1980: Continental stretching: an explanation of the post-mid-Cretaceous subsidence of the Central North Sea basin. *Journal of Geophysical Research 85*, 3711–3739.

Sclater, J. G., Hellinger, S. J. & Shorey, M. 1986: An analysis of the importance of extension in accounting for the post-Carboniferous subsidence of the North Sea basin. *University of Texas Institute for Geophysics Internal Report*. 25 pp.

Solli, M. 1976: *En seismisk skorpeundersokelse Norge-Shetland.* Unpublished thesis, University of Bergen.

Steckler, M. S. 1985: Uplift and extension at the Gulf of Suez: indications of induced mantle convection. *Nature 317*, 6033, 135–139.

Steckler, M. S. & Watts, A. B. 1978: Subsidence of the Atlantic-type continental margin off New York. *Earth & Planetary Science Letters 41*, 1–13.

Vail, P. R., Mitchum, R. M. & Thompson, S. 1977: Seismic stratigraphy and global changes in sea level, stratigraphic interpretation of seismic data. *American Association of Petroleum Geologists Memoir 26*, 83–97.

Van Hinte, J. E. 1978: Geohistory analysis – application of micropaleontology in exploration geology. *American Association of Petroleum Geologists Bulletin 62*, 2, 201–222.

Watts, A. B. 1982: Tectonic subsidence, flexure, and global changes of sea level. *Nature 297*, 469–474.

Watts, A. & Steckler, M. 1979: Subsidence and eustacy at the continental margin of eastern North America. *American Geophysical Union, Maurice Ewing series 3*, 218–234.

Wernicke, B. & Burchfiel, B. C. 1982: Modes of extensional tectonics. *Journal of Structural Geology 4*, 105–115.

White, N. J., Jackson, J. A. & McKenzie, D. P. (in press): The relationship between the geometry of normal faults and that of the sedimentary layers in their hanging walls. Submitted to *Journal of Structural Geology.*

Wood, R. J. 1981: The subsidence history of Conoco well 15/30–1, central North Sea. *Earth & Planetary Science Letters 54*, 306–312.

Ziegler, P. A. 1977: Geology and hydrocarbon provinces of the North Sea. *Geojournal 1*, 7–32.

Ziegler, P. A. 1981: Evolution of sedimentary basins in Northwest Europe. In Illing & Hobson (eds.): *Petroleum Geology of the Continental Shelf of NW Europe,* Heyden & Son, Ltd., London, 3–39.

Ziegler, P. A. 1982: *Geologic Atlas of Northwest Europe*, Shell Oil Company. 250 pp.

Ziegler, P. A. 1983: Crustal thinning and subsidence in the North Sea. *Nature 304*, 561.